

3. Magneto-optic Kerr effect (MOKE)

In this Chapter, after a brief introduction to the magneto-optic Kerr effect (MOKE) a phenomenological analysis of calibration methods for measuring the Kerr rotation, θ_K , and Kerr ellipticity, ε_K , will be described within the classical Jones matrix formalism. Novel compensation methods for absolute calibration of both Kerr quantities will be proposed and the experimental set-up of a polar Kerr spectrometer for ultra-high vacuum operation will be presented.

3.1. Phenomenology

The magneto-optic Kerr effect [Kerr76, 77] has attracted considerable interest in recent years because of its wide application in MO recording devices. Thanks to its high accuracy, high temporal and spatial resolution and very fast response the MO probe has become a powerful method to study the magnetic properties of ultrathin and multilayer films. Determination of electronic structure [Ersk73], observation of domains [Schm85], investigation of oscillations in the coupling between ferromagnetic layers via intercalated non-magnetic metallic layers [John92] and studies of two-dimensional Ising model behavior of ultrathin layers [Liu88, Kohl92] are some out of many examples.

The MOKE describes the change of the polarization states of light when reflected at a magnetic material. Thereby linearly polarized light experiences a rotation of the polarization plane, Kerr rotation θ_K , and a phase difference between the electric field components perpendicular and parallel to the plane of the incident light as described by the Kerr ellipticity, ε_K . These two quantities are connected to form the complex Kerr angle

$$\phi_K = \theta_K + i\varepsilon_K. \quad (3.1)$$

In a phenomenological description of MOKE the interaction of the magnetic sample with the electromagnetic field is represented by the dielectric tensor (DK) $\tilde{\varepsilon}$ [Argy55, Busc88], which yields

$$\phi_K = \theta_K + i\varepsilon_K = \frac{i\tilde{\varepsilon}_{xy}}{\sqrt{\tilde{\varepsilon}_{xx}(1-\tilde{\varepsilon}_{xx})}}. \quad (3.2)$$

$\tilde{\varepsilon}_{xx}$ and $\tilde{\varepsilon}_{xy}$ are diagonal and off-diagonal elements of the DK tensor, respectively. The off-diagonal elements of the DK tensor are linearly dependent on the magnetization and describe the magneto-optic contributions, which occur through different absorption of left and right circular polarized light. They are caused by spin orbit coupling and spin polarization. The diagonal elements describe optical reflectivity [Ersk73].

Because of the different magnetization directions relative to the plane of the incident light there are three different configurations for MOKE as depicted in Fig. 3.1 [Nede85]. In the polar Kerr effect configuration (a) the magnetization \mathbf{M} lies perpendicularly to the sample surfaces. In the case of longitudinal Kerr effect (b) \mathbf{M} lies parallel to the sample surfaces and to the plane of incidence. In the equatorial or transverse configuration (c) \mathbf{M} lies parallel to the sample surfaces and perpendicular to the plane of incidence.

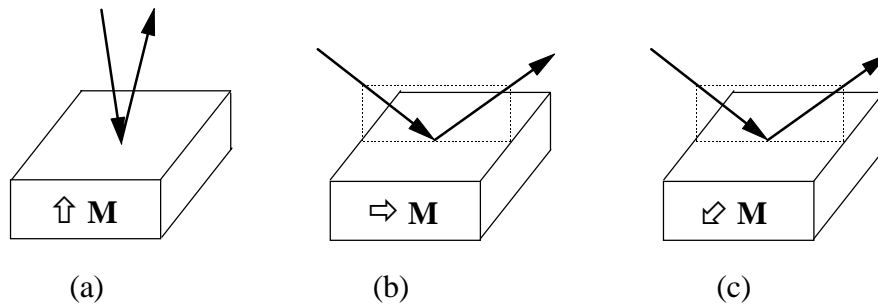


Fig. 3.1: Illustration of variant configurations for the magneto-optic Kerr effect

3.2. Calibration methods

The set-up for measuring polar Kerr optical quantities is schematically depicted in Fig. 3.2 (see Fig. 3.3). The optical elements consist of two Glan-Thomson-air polarizing prisms, **A** (analyzer) and **P** (polarizer), an elasto-optic modulator, **O**, and a calcite-wedge Babinet-Soleil type compensator, **C**. Furthermore, the direction of the linear components of the incident and reflected light vectors, $\mathbf{E}^i = (E_s^i, E_p^i)$ and $\mathbf{E}^r = (E_s^r, E_p^r)$, respectively, are depicted. The arrows in Fig. 3.2 represent the axes of the polarizers, **A** and **P**, and the neutral lines of the birefringent

elements, **O** and **C**, with respect to the *s* and *p* directions. These are perpendicular and parallel to the optical plane of the incident light on the sample **S**. **P** is fixed at an angle $\alpha = \pi/4$, whereas **A** is rotatable by an arbitrary angle β with respect to the *p* direction.

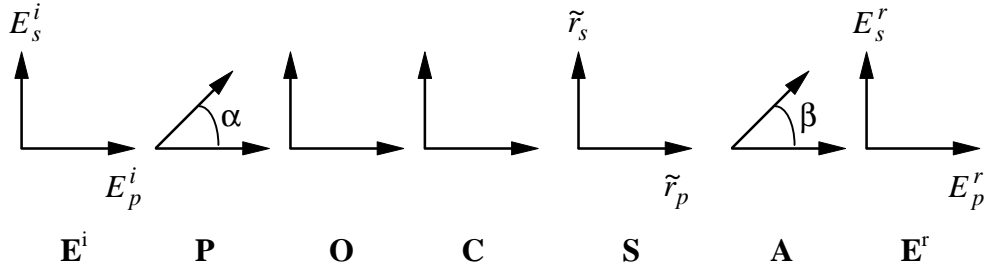


Fig. 3.2: Schematic description of the set-up for measuring magneto-optic Kerr effects (see text) and orientations of the light vector components ($E_s^i, E_p^i; E_s^r, E_p^r$), the polarizer axes (**A**, **P**) and the neutral directions of modulator (**O**) and compensator (**C**), depicted in planes normal to the light propagation and relative to the *s* and *p* directions defined by the plane of incidence and the sample surface (**S**).

Light transmission through the optical arrangement shown in Fig. 3.2 is described by the vector equation

$$\mathbf{E}^r = \mathbf{A} \cdot \mathbf{S} \cdot \mathbf{C} \cdot \mathbf{O} \cdot \mathbf{P} \cdot \mathbf{E}^i, \quad (3.3)$$

where

$$\mathbf{A} = \begin{pmatrix} \cos^2 \beta & \sin \beta \cos \beta \\ \sin \beta \cos \beta & \sin^2 \beta \end{pmatrix}, \quad (3.4)$$

$$\mathbf{S} = \begin{pmatrix} \tilde{r}_p & \tilde{r}_{ps} \\ \tilde{r}_{sp} & \tilde{r}_s \end{pmatrix} = \begin{pmatrix} r_p e^{i\delta_p} & r_{ps} e^{i\delta_{ps}} \\ r_{sp} e^{i\delta_{sp}} & r_s e^{i\delta_s} \end{pmatrix}, \quad (3.5)$$

$$\mathbf{C} = \begin{pmatrix} e^{i\frac{\gamma}{2}} & 0 \\ 0 & e^{-i\frac{\gamma}{2}} \end{pmatrix}, \quad (3.6)$$

$$\mathbf{O} = \begin{pmatrix} e^{i\frac{\varphi}{2}} & 0 \\ 0 & e^{-i\frac{\varphi}{2}} \end{pmatrix} \quad (3.7)$$

and

$$\mathbf{P} = \begin{pmatrix} 1/2 & 1/2 \\ 1/2 & 1/2 \end{pmatrix} \text{ with } \alpha = \frac{\pi}{4} \quad (3.8)$$

are the Jones matrices [Azza79] attributed to the elements **A**, **S**, **C**, **O** and **P**, respectively. Here all depolarization, reflection and absorption effects of the optical elements are neglected and perpendicular incidence on the optical elements is assumed.

The reflectivity of the sample, Eq. (3.5), is described in terms of the complex Fresnel coefficients, \tilde{r}_p and \tilde{r}_s , and the off-diagonal cross terms, \tilde{r}_{ps} and \tilde{r}_{sp} , which account for the MO Kerr effect [Nede85]. By distinguishing \tilde{r}_p from \tilde{r}_s the description holds at arbitrary angles of incidence. Hence the following treatment includes both polar and the longitudinal Kerr geometry (see Fig. 3.1). Here we note that

$$\tilde{r}_p = r_p \exp(i\delta_p), \quad (3.9)$$

$$\tilde{r}_s = r_s \exp(i\delta_s) \quad (3.10)$$

and, by symmetry,

$$\tilde{r}_{ps} = -\tilde{r}_{sp} = r_{ps} \exp(i\delta_{ps}) = -r_{sp} \exp(-i\delta_{sp}). \quad (3.11)$$

An additional phase shift will be achieved by a Babinet-Soleil type calcite wedge compensator, which will be used in particular as a $\lambda/4$ plate (see below). **O** and **C** are hit by the linearly polarized light at angles of $\pi/4$ with respect to their neutral lines. They exhibit temporally periodic function

$$\varphi(t) = \varphi_0 \sin(\omega_M t), \quad (3.12)$$

where the variable t denotes the time and should not be mistaken as a sample thickness as used in all Chapters except Chap. 3.

\mathbf{M} is driven at an angular frequency $\omega_M = 2\pi \cdot 50$ kHz with an amplitude $\varphi_0 \approx 2.41$.

Evaluation of Eq. (3. 3) is straightforward by inserting of Eqs. (3. 4 - 3. 8) into Eq. (3. 3):

$$\begin{aligned} \mathbf{E}^r = \frac{1}{2} \mathbf{E} \begin{pmatrix} \cos \beta \\ \sin \beta \end{pmatrix} & \left[e^{i\frac{1}{2}(\varphi+\gamma)} (\cos \beta r_p e^{i\delta_p} + \sin \beta r_{sp} e^{i\delta_{sp}}) + \right. \\ & \left. + e^{-i\frac{1}{2}(\varphi+\gamma)} (\sin \beta r_s e^{i\delta_s} - \cos \beta r_{sp} e^{i\delta_{sp}}) \right]; \quad \mathbf{E} = \mathbf{E}_s + \mathbf{E}_p. \end{aligned} \quad (3. 13)$$

The intensity of the reflected light behind \mathbf{A} is given by

$$I^r = (\mathbf{E}^r)^2 = \tilde{I} \frac{I^i}{2}, \quad (3. 14)$$

where I^i is the initial intensity

$$\mathbf{E}_p^i = \mathbf{E}_s^i = \sqrt{\frac{I^i}{2}}. \quad (3. 15)$$

For the amplitude \tilde{I} we obtain

$$\begin{aligned} \tilde{I} = & r_p^2 \cos^2 \beta + r_{sp}^2 \sin^2 \beta + r_p r_{sp} \sin 2\beta \cos(\delta_p - \delta_{sp}) + \\ & + r_s^2 \sin^2 \beta + r_{sp}^2 \cos^2 \beta - r_s r_{sp} \sin 2\beta \cos(\delta_s - \delta_{sp}) + \\ & + \cos(\varphi + \gamma) [r_s r_p \sin 2\beta \cos(\delta_p - \delta_s) - 2 r_p r_{sp} \cos^2 \beta \cos(\delta_p - \delta_{sp}) + \\ & + 2 r_s r_{sp} \sin^2 \beta \cos(\delta_s - \delta_{sp}) - r_{sp}^2 \sin 2\beta] + \end{aligned} \quad (3. 16)$$

$$\begin{aligned} & + \sin(\varphi + \gamma) [r_s r_p \sin 2\beta \sin(\delta_s - \delta_p) + \\ & + 2 r_p r_{sp} \cos^2 \beta \sin(\delta_p - \delta_{sp}) + 2 r_s r_{sp} \sin^2 \beta \sin(\delta_s - \delta_{sp})] \\ = & r_p^2 \cos^2 \beta + r_s^2 \sin^2 \beta + r_{sp}^2 + \\ & + r_{sp} \sin 2\beta [r_p \cos(\delta_p - \delta_{sp}) - r_s \cos(\delta_s - \delta_{sp})] + \\ & + \cos(\varphi + \gamma) [\sin 2\beta \{r_s r_p \cos(\delta_p - \delta_s) - r_{sp}^2\} + \\ & + 2 r_{sp} \{r_s \sin^2 \beta \cos(\delta_s - \delta_{sp}) + \cos^2 \beta \cos(\delta_p - \delta_{sp})\}] + \\ & + \sin(\varphi + \gamma) [r_s r_p \sin 2\beta \sin(\delta_s - \delta_p) + \\ & + 2 r_{sp} \{r_s \sin^2 \beta \sin(\delta_s - \delta_{sp}) + r_p \cos^2 \beta \sin(\delta_p - \delta_{sp})\}]. \end{aligned} \quad (3. 17)$$

In order to simplify Eq. (3. 17) we define the following substitutions:

$$A = r_p^2 \cos^2 \beta + r_s^2 \sin^2 \beta + r_{sp}^2 + r_{sp} \sin 2\beta [r_p \cos(\delta_p - \delta_{sp}) - r_s \cos(\delta_s - \delta_{sp})], \quad (3. 18)$$

$$B = [\sin 2\beta \{r_s r_p \cos(\delta_p - \delta_s) - r_{sp}^2\} + 2 r_{sp} \{r_s \sin^2 \beta \cos(\delta_s - \delta_{sp}) + \cos^2 \beta \cos(\delta_p - \delta_{sp})\}], \quad (3. 19)$$

$$C = [r_s r_p \sin 2\beta \sin(\delta_s - \delta_p) + 2 r_{sp} \{r_s \sin^2 \beta \sin(\delta_s - \delta_{sp}) + r_p \cos^2 \beta \sin(\delta_p - \delta_{sp})\}]. \quad (3. 20)$$

Hence we obtain the following equation

$$\tilde{I} = A + \cos(\varphi + \gamma)B + \sin(\varphi + \gamma)C. \quad (3. 21)$$

The terms $\cos(\varphi + \gamma)$ and $\sin(\varphi + \gamma)$ are solved by the trigonometric relations

$$\cos(\varphi + \gamma) = \cos \varphi \cos \gamma - \sin \varphi \sin \gamma \quad (3. 22)$$

and

$$\sin(\varphi + \gamma) = \cos \varphi \sin \gamma + \sin \varphi \cos \gamma. \quad (3. 23)$$

In view of the lock-in technique employed only the lowest Fourier components of relation Eq. (3. 21) are of interest. They are deduced from

$$\sin \varphi = \sin(\varphi_0 \sin \omega_M t) = J_1(\varphi_0) \sin \omega_M t + 2 J_3(\varphi_0) \sin 3\omega_M t + \dots \quad (3. 24)$$

and

$$\cos \varphi = \cos(\varphi_0 \sin \omega_M t) = J_0(\varphi_0) + 2 J_2(\varphi_0) \cos 2\omega_M t + \dots, \quad (3. 25)$$

where $J_k(k = 0, 1, 2, \dots)$ are Bessel's functions of order k . By use of the relations (3. 22) and (3. 23) we may rewrite Eq. (3. 21) as

$$\tilde{I} = \tilde{I}_0 + \tilde{I}_\omega \sin \omega_M t + \tilde{I}_{2\omega} \cos 2\omega_M t + O(3\omega_M t) \quad (3. 26)$$

with the expansion coefficients

$$\tilde{I}_0 = A + J_0(\varphi_0)[\cos \gamma \cdot B + \sin \gamma \cdot C], \quad (3.27)$$

$$\tilde{I}_\omega = 2 J_1(\varphi_0)[\cos \gamma \cdot C - \sin \gamma \cdot B], \quad (3.28)$$

$$\tilde{I}_{2\omega} = 2 J_2(\varphi_0)[\cos \gamma \cdot B + \sin \gamma \cdot C]. \quad (3.29)$$

By choosing specific settings of γ and β the Eqs. (3.18 - 20) and (3.27 - 29) can considerably be simplified. For the general case of oblique incidence, we notice the solutions for two important cases. They were discussed previously [Nede85] with slight modifications.

(i) p-polarisation: $\gamma = 0$, $\beta = 0$

$$\tilde{I}_0 = r_p^2 + r_{sp}^2 - 2 J_0(\varphi_0) r_{sp} r_p \cos(\delta_p - \delta_{sp}), \quad (3.30)$$

$$\tilde{I}_\omega = 4 J_1(\varphi_0) r_{sp} r_p \sin(\delta_p - \delta_{sp}), \quad (3.31)$$

$$\tilde{I}_{2\omega} = -4 J_2(\varphi_0) r_{sp} r_p \cos(\delta_p - \delta_{sp}), \quad (3.32)$$

(ii) s-polarisation: $\gamma = 0$, $\beta = \pi/2$

$$\tilde{I}_0 = r_s^2 + r_{sp}^2 + 2 J_0(\varphi_0) r_{sp} r_s \cos(\delta_s - \delta_{sp}), \quad (3.33)$$

$$\tilde{I}_\omega = 4 J_1(\varphi_0) r_{sp} r_s \sin(\delta_s - \delta_{sp}), \quad (3.34)$$

$$\tilde{I}_{2\omega} = 4 J_2(\varphi_0) r_{sp} r_s \cos(\delta_s - \delta_{sp}). \quad (3.35)$$

The Kerr rotation θ_K and ellipticity ε_K are defined by [Klei88]

$$\theta_s = \frac{r_{sp}}{r_s} \cos(\delta_s - \delta_{sp}), \quad (3.36)$$

$$\theta_p = \frac{r_{ps}}{r_p} \cos(\delta_p - \delta_{sp}), \quad (3.37)$$

and

$$\tan \varepsilon_s = -\frac{r_{sp}}{r_s} \sin(\delta_s - \delta_{sp}), \quad (3.38)$$

$$\tan \varepsilon_p = \frac{r_{ps}}{r_p} \sin(\delta_p - \delta_{sp}). \quad (3.39)$$

Since $J_0(\varphi_0) \approx 0$ at $\varphi_0 \approx 2.41$, and $r_{sp}^2 \ll r_p^2, r_s^2$ and taking into account the definitions of θ_K and ϵ_K , Eqs. (3. 36 - 39), one readily obtains the ratios

$$\left(\frac{\tilde{I}_{2\omega}}{\tilde{I}_0}\right)_{\beta=0} = -4 J_2(\varphi_0) \frac{r_{sp}}{r_p} \cos(\delta_p - \delta_{sp}) = -4 J_2(\varphi_0) \theta_p, \quad (3. 40)$$

$$\left(\frac{\tilde{I}_{2\omega}}{\tilde{I}_0}\right)_{\beta=\pi/2} = 4 J_2(\varphi_0) \frac{r_{sp}}{r_s} \cos(\delta_p - \delta_{sp}) = 4 J_2(\varphi_0) \theta_s, \quad (3. 41)$$

$$\left(\frac{\tilde{I}_\omega}{\tilde{I}_0}\right)_{\beta=0} = 4 J_1(\varphi_0) \frac{r_{sp}}{r_p} \sin(\delta_p - \delta_{sp}) = 4 J_1(\varphi_0) \tan \epsilon_p, \quad (3. 42)$$

$$\left(\frac{\tilde{I}_\omega}{\tilde{I}_0}\right)_{\beta=\pi/2} = 4 J_1(\varphi_0) \frac{r_{sp}}{r_s} \cos(\delta_s - \delta_{sp}) = 4 J_1(\varphi_0) \tan \epsilon_s. \quad (3. 43)$$

We restrict ourselves to the polar Kerr configuration at near perpendicular incidence owing to the geometry of our experimental set-up (see Fig. 3.3). By setting

$$r_p = r_s = r, \quad \delta_p = \delta_s = \delta, \quad (3. 44)$$

Eqs. (3. 18 -20) have to be replaced by

$$A' = r^2 + r_{sp}^2, \quad (3. 45)$$

$$B' = \sin 2\beta(r^2 - r_{sp}^2) - 2r r_{sp} \cos 2\beta \cos(\delta - \delta_{sp}), \quad (3. 46)$$

$$C' = 2r r_{sp} \sin(\delta - \delta_{sp}). \quad (3. 47)$$

Hence, apart from numerical factors the normalized lock-in signals at ω_M and ω_{2M} directly yield the Kerr rotations and ellipticities, respectively. In addition, by taking ratios of two light intensity signals, fluctuations due to instabilities of the light source (intensity \tilde{I} , Eq. 3. 15) and of the optical set-up are very efficiently eliminated. In practice, recording of the signals (3. 40 - 43) requires two different amplifiers with unknown additional proportionality constants. There are two calibration methods, which are referred to as the two-angle and the compensation methods in the following. They are used to determine the absolute values of the Kerr quantities [Kim93]. Here we will discuss only the compensation method, which is applied in all of our further

investigations. Details of the alternative calibration method, the two-angle method, were discussed elsewhere [Kim93].

3.2.1. Calibration of the Kerr rotation θ_K

Inspection of Eq. (3. 29) yields a procedure for a calibrated measurement of θ_K . Set $\gamma = 0$ and $\beta \approx 0$, and compensate for $\tilde{I}_{2\omega}$ by controlling β

$$\begin{aligned}\tilde{I}_{2\omega} &= 2 J_2(\varphi_0)B \\ &= 2 J_2(\varphi_0)[\sin 2\beta(r^2 - r_{sp}^2) - 2r r_{sp} \cos 2\beta \cos(\delta - \delta_{sp})].\end{aligned}\tag{3. 48}$$

Since $r^2 \gg r_{sp}^2$ and $\tan 2\beta \approx 2\beta$ one obtains

$$\tilde{I}_{2\omega} = 2 J_2(\varphi_0)[\sin 2\beta(r^2 - r_{sp}^2) - 2r r_{sp} \cos 2\beta \cos(\delta - \delta_{sp})] = 0,\tag{3. 49}$$

$$\Rightarrow \frac{1}{2} \frac{\sin 2\beta}{\cos 2\beta} = \frac{r_{sp}}{r} \cos(\delta - \delta_{sp}) = \theta_k, r^2 \gg r_{sp}^2\tag{3. 50}$$

$$\Rightarrow \frac{1}{2} \tan 2\beta \approx \beta = \theta_k.$$

This approximation is valid for small angles β . Eq. (3. 50) shows that the orientation β of the analyzer **A** immediately yields θ_K . Absolutely calibrated data, e. g. hysteresis cycles θ_K vs. H , may thus be recorded point-by-point. After recording $\tilde{I}_{2\omega}$ data at $\beta = 0$, which are proportional to θ_K , one simply calibrates $\tilde{I}_{2\omega}$ axis by taking $\tilde{I}_{2\omega}$ values at distinct steps of β with fixed θ_K (e. g. at $H = 0$). According to Eq. (3. 49) the β steps chosen correspond to equally sized steps of θ_K . A similar calibration procedure was proposed previously [Sato81].

3.2.2. Calibration of the Kerr ellipticity ϵ_K

In order to calibrate the Kerr ellipticity one needs circular polarized light. This can be realized by inserting a $\lambda/4$ plate by virtue of the Babint-Soleil compensator into the optical path.

Analogously to the Kerr rotation again a compensation method is applied. Inspection of Eqs. (3. 28), (3. 46) and (3. 47) yields a procedure for calibrated measurements of ϵ_K .

$$\begin{aligned} \tilde{I}_\omega = 2 J_1(\omega) [\cos \gamma \{ 2r r_{sp} \sin(\delta - \delta_{sp}) \} - \\ - \sin \gamma \{ \sin 2\beta (r^2 - r_{sp}^2) - 2r r_{sp} \cos 2\beta \cos(\delta - \delta_{sp}) \}] = 0. \end{aligned} \quad (3. 51)$$

Set $\beta = \pi/4$, $\gamma \approx 0$ and compensate for \tilde{I}_w by controlling γ

$$\tilde{I}(\gamma \approx 0, \beta = \frac{\pi}{4}) = \cos \gamma [2r r_{sp} \sin(\delta - \delta_{sp})] - \sin \gamma [r^2 - r_{sp}^2] = 0 \quad (3. 52)$$

$$\Rightarrow \frac{1}{2} \tan \gamma = \frac{r_{sp}}{r} \sin(\delta - \delta_{sp}) = \tan \epsilon_k; \quad r^2 \gg r_{sp}^2 \quad (3. 53)$$

$$\Rightarrow \frac{1}{2} \gamma = \epsilon_k, \quad \gamma \text{ and } \epsilon_k \ll 1.$$

Hence the phase shift of the compensator **C** immediately yields $2\epsilon_K$ (in radians). Again, Eq. (3. 53) suggests either to record ϵ_K by compensating \tilde{I}_w point-by-point, or to calibrate the \tilde{I}_w scale with distinct steps of γ at fixed ϵ_K (e.g. at $H = 0$).

One advantage of the compensation methods, Eqs. (3. 50) and (3. 53), is their inherent insensitivity against fluctuations of the light intensity. As experienced in conventional methods, Eq. (3. 40 - 43), it is strongly suggested to normalize all data with the dc signal recorded simultaneously (see Chapter 3. 3). One thus cancels the influence of fluctuations of I^i (see Eq. 3. 14). It has to be noticed, however, that this mode strictly requires $\varphi_0 = 2.41$ in order to obtain $J_0(\varphi_0) = 0$. Only by this measure unwanted dependence of the normalizing factor \tilde{I}_0 on variations of β or γ is avoided.